

Formation and structure of the ferryl [Fe=O] intermediate in the non-haem iron halogenase SyrB2: classical and QM/MM modelling agree

G. Rugg and H. M. Senn

WestCHEM and School of Chemistry, University of Glasgow, Glasgow G12 8QQ, UK

1 Supplementary Computational Details

1.1 Protein structure preparation

The complete protein structure was prepared by A. Jarnuczak¹ using the program Modeller^{2,3}, which creates potential structures for missing loops by constructing an initial loop model, randomly displacing it to generate a number of structures, then carrying out an optimisation of each of these structures at the MM level. 100 such optimised structures were generated, and the most favourable selected according to its DOPE-HR⁴ score and its RMSD from 2FCT. Next, hydrogen atoms were added and Asn/Gln/His residues checked for flips using Reduce^{5,6} via the MolProbity server⁷. The residues Gln11, Asn95, Gln129, and Gln245 were flipped from their conformation in the crystal structure. Finally, the protonation states of all titratable residues were calculated using PropKa^{8,9}. Protonation states of histidine residues are shown in Table S1; all other residues were left in their standard protonation states.

Table S1: Protonation states of histidine residues

Residue	Protonation State
His69	N ^e
His78	N ^e
His116	N ^d
His235	N ^d
His240	N ^e
His261	N ^d
His268	N ^e
His300	N ^e

1.2 QM calculations on model compounds, atomic charges for non-standard residues

Partial charges for non-standard residues were obtained at the DFT level by fitting to the molecular electrostatic potential according to the Merz–Singh–Kollmann scheme¹⁰; structures were fully optimised at the same level of theory unless indicated otherwise. For compatibility with the Amber ff03 force field¹¹, charges were determined in a polarisable continuum solvent. For the singlet Fe(II) complexes, charges were taken from TPSS-D/def2-TZVP/COSMO($\epsilon = 80$) calculations run with TURBOMOLE^{12–14}; charges for the Fe(IV) complexes in the quintet state from B3LYP/def2-TZVP+/PCM($\epsilon = 3.9$) calculations in Gaussian¹⁵; and charges for the substrates from B97-D/def2-TZVP/PCM(water) calculations with Gaussian. For **ABA** and **NVA**, a distance constraint was used to ensure that the pantetheine was in the same extended conformation as for **THR**. It was verified that the slightly different choices of exchange–correlation functional and value of ϵ had negligible effect on the fitted charges.

For residues cut by a QM–MM boundary, the charges were corrected such as to ensure that the total charge of the atoms that would become QM atoms summed up to an integer value; by construction, the total charge of the remaining MM atoms is then also an integer value. The corrections required to ensure charge integrity were small; the imbalance was distributed over all atoms of the residue, leading to very small ($< 0.01e$) changes of the original atomic charges.

1.3 MD simulations

1.3.1 Simulation parameters

MD simulations were run under periodic boundary conditions in a rhombic-dodecahedral box with an image distance of $d \approx 7.88$ nm, chosen to give a minimal simulation volume while maintaining a minimum distance of 1 nm to the solute. The simulation systems were neutralised by the addition of counterions (14 Na⁺ for systems containing substrate). Electrostatic interactions were treated with the particle–mesh Ewald (PME) method ($r_C = 1.0$ nm, fourth-order interpolation, tolerance 10^{-5} , grid spacing 0.12 nm). Van der Waals interactions were cut off at $r_{vdW} = 1.0$ nm. Energies and pressures were corrected for long-range dispersion effects.

The simulation stages and parameters are summarised in Table S2. A time step of 2 fs was used throughout. Overall equilibration was judged by convergence of the backbone RMSD according to a series of statistical tests^{16,17}. The production runs were continued to about 20 ns or until conformational equilibration for the active site residues was established. Each trajectory spanned up to 40 ns in total.

Table S2: Equilibration procedure for MD simulations with Fe(II) active-site complex

Parameter	Energy Minimisation	Temperature Equilibration	Equilibration Stage 1	Equilibration Stage 2	Equilibration Stage 3	Final Equilibration/Production
Ensemble Integrator	— Steepest descent	NVT	NPT	NPT Leap-frog	NPT	NVT
Duration (ps)	—	100	400	100 all bonds	400	until equilibration
Constraints	all bonds to hydrogen					
Position restraints on non-H (kJ mol ⁻¹ nm ⁻¹)	1000	1000	1000	100	0	0
τ_T (ps)	—	0.1	0.1	0.1	0.1	2
τ_p (ps)	—	—	1	1	1	—

1.3.2 Force-field parameters

For the residues containing atoms with non-standard charges, we list here the [atoms] blocks in GROMACS topology format. All atom types (and therefore van der Waals parameters) were standard atom types from either Amber ff03 or GAFF.

A-H₂O

```
; id      at type      res nr  residu name      at name  cg nr  charge
1       FE           1        IRO          IRO        1      0.784449

; id      at type      res nr  residu name      at name  cg nr  charge
1       Cl           1        CLO          CLO        1     -0.706289

; AKG = 20G
;   nr  type  resi  res  atom  cgnr  charge    mass      ; qtot
  1   c   1209  AKG    C    1   0.771763  12.01000 ; qtot -0.083
  2   o   1209  AKG    O    2  -0.683526  16.00000 ; qtot -0.184
  3   o   1209  AKG    O1   3   -0.70403  16.00000 ; qtot -0.252
  4   c   1209  AKG    C1   4   0.328831  12.01000 ; qtot -0.319
  5   o   1209  AKG    O2   5   -0.446477  16.00000 ; qtot -0.375
  6   c3  1209  AKG    C2   6   -0.050528  12.01000 ; qtot -0.469
  7   c3  1209  AKG    C3   7   -0.055613  12.01000 ; qtot -0.551
  8   c   1209  AKG    C4   8   0.856546  12.01000 ; qtot -0.655
  9   o   1209  AKG    O3   9   -0.869579  16.00000 ; qtot -0.752
 10   o   1209  AKG    O4  10   -0.829547  16.00000 ; qtot -0.649
 11   hc  1209  AKG    H  11   -0.007143  1.00800 ; qtot -0.760
 12   hc  1209  AKG    H1  12   -0.002513  1.00800 ; qtot -0.862
 13   hc  1209  AKG    H2  13   0.030762  1.00800 ; qtot -0.931
 14   hc  1209  AKG    H3  14   0.069932  1.00800 ; qtot -1.000

; VOD = coordinated water
; id  at type  res nr  res name  at name  cg nr  charge  mass
```

1	OW	1	VOD	OW	1	-0.799831	16.00000
2	HW	1	VOD	HW1	1	0.378185	1.00800
3	HW	1	VOD	HW2	1	0.42859	1.00800

; residue 116 HIQ rtp HIQ q 0.0

1816	N	116	HIQ	N	1816	-0.506799	14.01 ; qtot -4.507
1817	H	116	HIQ	H	1817	0.351021	1.008 ; qtot -4.156
1818	CT	116	HIQ	CA	1818	0.119066	12.01 ; qtot -4.037
1819	H1	116	HIQ	HA	1819	0.137761	1.008 ; qtot -3.899
1820	CT	116	HIQ	CB	1820	-0.122638	12.01 ; qtot -4.022
1821	HC	116	HIQ	HB1	1821	0.086329	1.008 ; qtot -3.935
1822	HC	116	HIQ	HB2	1822	0.086329	1.008 ; qtot -3.849
1823	CC	116	HIQ	CG	1823	0.340433	12.01 ; qtot -3.85
1824	NA	116	HIQ	ND1	1824	-0.340626	14.01 ; qtot -4.056
1825	H	116	HIQ	HD1	1825	0.349008	1.008 ; qtot -3.738
1826	CR	116	HIQ	CE1	1826	-0.085004	12.01 ; qtot -3.591
1827	H5	116	HIQ	HE1	1827	0.175775	1.008 ; qtot -3.469
1828	NB	116	HIQ	NE2	1828	-0.117347	14.01 ; qtot -4.07
1829	CV	116	HIQ	CD2	1829	-0.354558	12.01 ; qtot -4.026
1830	H4	116	HIQ	HD2	1830	0.156461	1.008 ; qtot -3.916
1831	C	116	HIQ	C	1831	0.515947	12.01 ; qtot -3.4
1832	O	116	HIQ	O	1832	-0.599831	16 ; qtot -4

; residue 235 HIX rtp HIX q 0.0

3655	N	235	HIX	N	3655	-0.506799	14.01 ; qtot -10.51
3656	H	235	HIX	H	3656	0.351021	1.008 ; qtot -10.16
3657	CT	235	HIX	CA	3657	0.119066	12.01 ; qtot -10.04
3658	H1	235	HIX	HA	3658	0.137761	1.008 ; qtot -9.899
3659	CT	235	HIX	CB	3659	-0.122638	12.01 ; qtot -10.02
3660	HC	235	HIX	HB1	3660	0.086329	1.008 ; qtot -9.935
3661	HC	235	HIX	HB2	3661	0.086329	1.008 ; qtot -9.849
3662	CC	235	HIX	CG	3662	0.314181	12.01 ; qtot -9.85
3663	NA	235	HIX	ND1	3663	-0.307132	14.01 ; qtot -10.06
3664	H	235	HIX	HD1	3664	0.350125	1.008 ; qtot -9.738
3665	CR	235	HIX	CE1	3665	-0.201184	12.01 ; qtot -9.591
3666	H5	235	HIX	HE1	3666	0.199216	1.008 ; qtot -9.469
3667	NB	235	HIX	NE2	3667	0.134339	14.01 ; qtot -10.07
3668	CV	235	HIX	CD2	3668	-0.428564	12.01 ; qtot -10.03
3669	H4	235	HIX	HD2	3669	0.186526	1.008 ; qtot -9.916
3670	C	235	HIX	C	3670	0.515947	12.01 ; qtot -9.4
3671	O	235	HIX	O	3671	-0.599831	16 ; qtot -10

A

;	id	at	type	res	nr	residu	name	at	name	cg	nr	charge
---	----	----	------	-----	----	--------	------	----	------	----	----	--------

1	FE			1		IRO		IRO		1		0.69874
---	----	--	--	---	--	-----	--	-----	--	---	--	---------

;	id	at	type	res	nr	residu	name	at	name	cg	nr	charge
---	----	----	------	-----	----	--------	------	----	------	----	----	--------

1	C1			1		CLO		CLO		1		-0.64616
---	----	--	--	---	--	-----	--	-----	--	---	--	----------

; AKG = 20G

;	nr	type	resi	res	atom	cgnr	charge	mass	;	qtot
1	c	1209	AKG	C	1	0.700254	12.01000	;	qtot	-0.111771
2	o	1209	AKG	O	2	-0.663076	16.00000	;	qtot	-0.133799
3	o	1209	AKG	O1	3	-0.634775	16.00000	;	qtot	-0.100448
4	c	1209	AKG	C1	4	0.376036	12.01000	;	qtot	-0.094001
5	o	1209	AKG	O2	5	-0.451993	16.00000	;	qtot	-0.071065
6	c3	1209	AKG	C2	6	-0.084148	12.01000	;	qtot	-0.105823
7	c3	1209	AKG	C3	7	-0.053219	12.01000	;	qtot	-0.080459
8	c	1209	AKG	C4	8	0.860231	12.01000	;	qtot	-0.099629
9	o	1209	AKG	O3	9	-0.870025	16.00000	;	qtot	-0.130951

```

10   o  1209   AKG   04   10   -0.828007    16.00000 ; qtot -0.081349
11   hc 1209   AKG     H   11   -0.006638    1.00800 ; qtot -0.06559
12   hc 1209   AKG     H1   12   -0.004849    1.00800 ; qtot -0.060775
13   hc 1209   AKG     H2   13    0.04114    1.00800 ; qtot -0.129752
14   hc 1209   AKG     H3   14    0.076491    1.00800 ; qtot -0.115577

; residue 116 HIQ rtp HIQ q 0.0
1816      N  116   HIQ      N  1816  -0.506799    14.01 ; qtot -4.507
1817      H  116   HIQ      H  1817  0.351021    1.008 ; qtot -4.156
1818      CT 116   HIQ     CA  1818  0.119066   12.01 ; qtot -4.037
1819      H1 116   HIQ     HA  1819  0.137761   1.008 ; qtot -3.899
1820      CT 116   HIQ     CB  1820  -0.122638   12.01 ; qtot -4.022
1821      HC 116   HIQ    HB1  1821  0.086329   1.008 ; qtot -3.935
1822      HC 116   HIQ    HB2  1822  0.086329   1.008 ; qtot -3.849
1823      CC 116   HIQ     CG  1823  0.357995   12.01 ; qtot -3.85
1824      NA 116   HIQ    ND1  1824  -0.349642   14.01 ; qtot -4.056
1825      H  116   HIQ    HD1  1825  0.353283   1.008 ; qtot -3.738
1826      CR 116   HIQ    CE1  1826  -0.11849   12.01 ; qtot -3.591
1827      H5 116   HIQ    HE1  1827  0.191526   1.008 ; qtot -3.469
1828      NB 116   HIQ    NE2  1828  -0.042566   14.01 ; qtot -4.07
1829      CV 116   HIQ    CD2  1829  -0.392046   12.01 ; qtot -4.026
1830      H4 116   HIQ    HD2  1830  0.181364   1.008 ; qtot -3.916
1831      C  116   HIQ     C  1831  0.515947   12.01 ; qtot -3.4
1832      O  116   HIQ     O  1832  -0.599831    16 ; qtot -4

; residue 235 HIX rtp HIX q 0.0
3655      N  235   HIX      N  3655  -0.506799    14.01 ; qtot -10.51
3656      H  235   HIX      H  3656  0.351021    1.008 ; qtot -10.16
3657      CT 235   HIX     CA  3657  0.119066   12.01 ; qtot -10.04
3658      H1 235   HIX     HA  3658  0.137761   1.008 ; qtot -9.899
3659      CT 235   HIX     CB  3659  -0.122638   12.01 ; qtot -10.02
3660      HC 235   HIX    HB1  3660  0.086329   1.008 ; qtot -9.935
3661      HC 235   HIX    HB2  3661  0.086329   1.008 ; qtot -9.849
3662      CC 235   HIX     CG  3662  0.303336   12.01 ; qtot -9.85
3663      NA 235   HIX    ND1  3663  -0.329661   14.01 ; qtot -10.06
3664      H  235   HIX    HD1  3664  0.347334   1.008 ; qtot -9.738
3665      CR 235   HIX    CE1  3665  -0.031523   12.01 ; qtot -9.591
3666      H5 235   HIX    HE1  3666  0.143737   1.008 ; qtot -9.469
3667      NB 235   HIX    NE2  3667  -0.11523   14.01 ; qtot -10.07
3668      CV 235   HIX    CD2  3668  -0.294443   12.01 ; qtot -10.03
3669      H4 235   HIX    HD2  3669  0.15065   1.008 ; qtot -9.916
3670      C  235   HIX     C  3670  0.515947   12.01 ; qtot -9.4
3671      O  235   HIX     O  3671  -0.599831    16 ; qtot -10

```

Substrate-D1

```

; id      at type          res nr  residu name      at name  cg nr  charge
1       FE              1        FER           IRO      1    0.684248
2       O               1        FER           FEO      1   -0.445369

; id      at type          res nr  residu name      at name  cg nr  charge
1       Cl              1        CLO           CLO      1   -0.531291

;      nr  type  resi  res  atom  cgnr      charge      mass      ; qtot
  1   o    1    SUC   0    1   -0.636592  16.00000 ; qtot -0.246
  2   c    1    SUC   C   2    0.598324  12.01000 ; qtot 0.110
  3   o    1    SUC   O1   3   -0.345319  16.00000 ; qtot -0.136
  4   c3   1    SUC   C1   4   -0.127374  12.01000 ; qtot -0.077
  5   c3   1    SUC   C2   5   -0.056894  12.01000 ; qtot -0.017
  6   c    1    SUC   C3   6    0.862099  12.01000 ; qtot 0.339
  7   o    1    SUC   O2   7   -0.882571  16.00000 ; qtot 0.093
  8   o    1    SUC   O3   8   -0.812840  16.00000 ; qtot -0.154

```

9	hc	1	SUC	H	9	-0.007683	1.00800 ; qtot -0.115
10	hc	1	SUC	H1	10	0.017870	1.00800 ; qtot -0.077
11	hc	1	SUC	H2	11	0.030399	1.00800 ; qtot -0.038
12	hc	1	SUC	H3	12	0.029686	1.00800 ; qtot -0.000
;							
; residue 116 HIQ rtp HIQ q 0.0							
1816	N	116	HIQ	N	1816	-0.506799	14.01 ; qtot -4.507
1817	H	116	HIQ	H	1817	0.351021	1.008 ; qtot -4.156
1818	CT	116	HIQ	CA	1818	0.119066	12.01 ; qtot -4.037
1819	H1	116	HIQ	HA	1819	0.137761	1.008 ; qtot -3.899
1820	CT	116	HIQ	CB	1820	-0.122638	12.01 ; qtot -4.022
1821	HC	116	HIQ	HB1	1821	0.086329	1.008 ; qtot -3.935
1822	HC	116	HIQ	HB2	1822	0.086329	1.008 ; qtot -3.849
1823	CC	116	HIQ	CG	1823	0.358772	12.01 ; qtot -3.85
1824	NA	116	HIQ	ND1	1824	-0.372509	14.01 ; qtot -4.056
1825	H	116	HIQ	HD1	1825	0.361030	1.008 ; qtot -3.738
1826	CR	116	HIQ	CE1	1826	0.020964	12.01 ; qtot -3.591
1827	H5	116	HIQ	HE1	1827	0.157317	1.008 ; qtot -3.469
1828	NB	116	HIQ	NE2	1828	-0.115046	14.01 ; qtot -4.07
1829	CV	116	HIQ	CD2	1829	-0.332913	12.01 ; qtot -4.026
1830	H4	116	HIQ	HD2	1830	0.178074	1.008 ; qtot -3.916
1831	C	116	HIQ	C	1831	0.515947	12.01 ; qtot -3.4
1832	O	116	HIQ	O	1832	-0.599831	16 ; qtot -4
;							
; residue 235 HIX rtp HIX q 0.0							
3655	N	235	HIX	N	3655	-0.506799	14.01 ; qtot -10.51
3656	H	235	HIX	H	3656	0.351021	1.008 ; qtot -10.16
3657	CT	235	HIX	CA	3657	0.119066	12.01 ; qtot -10.04
3658	H1	235	HIX	HA	3658	0.137761	1.008 ; qtot -9.899
3659	CT	235	HIX	CB	3659	-0.122638	12.01 ; qtot -10.02
3660	HC	235	HIX	HB1	3660	0.086329	1.008 ; qtot -9.935
3661	HC	235	HIX	HB2	3661	0.086329	1.008 ; qtot -9.849
3662	CC	235	HIX	CG	3662	0.362487	12.01 ; qtot -9.85
3663	NA	235	HIX	ND1	3663	-0.401630	14.01 ; qtot -10.06
3664	H	235	HIX	HD1	3664	0.354126	1.008 ; qtot -9.738
3665	CR	235	HIX	CE1	3665	0.006603	12.01 ; qtot -9.591
3666	H5	235	HIX	HE1	3666	0.146663	1.008 ; qtot -9.469
3667	NB	235	HIX	NE2	3667	-0.098290	14.01 ; qtot -10.07
3668	CV	235	HIX	CD2	3668	-0.366903	12.01 ; qtot -10.03
3669	H4	235	HIX	HD2	3669	0.230197	1.008 ; qtot -9.916
3670	C	235	HIX	C	3670	0.515947	12.01 ; qtot -9.4
3671	O	235	HIX	O	3671	-0.599831	16 ; qtot -10

Substrate-D2

;	id	at	type	res	nr	residu	name	at	name	cg	nr	charge	
1	FE			1		FER		IRO		1		0.684248	
2	O			1		FER		FEO		1		-0.445369	
;	id	at	type	res	nr	residu	name	at	name	cg	nr	charge	
1	Cl			1		CLO		CLO		1		-0.531291	
;	nr	type	resi	res	atom	cgnr	charge	mass				;	qtot
1	o	1	SUC	O	1	-0.636592	16.00000		qtot	-0.246			
2	c	1	SUC	C	2	0.598324	12.01000		qtot	0.110			
3	o	1	SUC	O1	3	-0.345319	16.00000		qtot	-0.136			
4	c3	1	SUC	C1	4	-0.127374	12.01000		qtot	-0.077			
5	c3	1	SUC	C2	5	-0.056894	12.01000		qtot	-0.017			
6	c	1	SUC	C3	6	0.862099	12.01000		qtot	0.339			
7	o	1	SUC	O2	7	-0.882571	16.00000		qtot	0.093			
8	o	1	SUC	O3	8	-0.812840	16.00000		qtot	-0.154			
9	hc	1	SUC	H	9	-0.007683	1.00800		qtot	-0.115			

```

10 hc 1 SUC H1 10 0.017870 1.00800 ; qtot -0.077
11 hc 1 SUC H2 11 0.030399 1.00800 ; qtot -0.038
12 hc 1 SUC H3 12 0.029686 1.00800 ; qtot -0.000

; residue 116 HIQ rtp HIQ q 0.0
1816 N 116 HIQ N 1816 -0.506799 14.01 ; qtot -4.507
1817 H 116 HIQ H 1817 0.351021 1.008 ; qtot -4.156
1818 CT 116 HIQ CA 1818 0.119066 12.01 ; qtot -4.037
1819 H1 116 HIQ HA 1819 0.137761 1.008 ; qtot -3.899
1820 CT 116 HIQ CB 1820 -0.122638 12.01 ; qtot -4.022
1821 HC 116 HIQ HB1 1821 0.086329 1.008 ; qtot -3.935
1822 HC 116 HIQ HB2 1822 0.086329 1.008 ; qtot -3.849
1823 CC 116 HIQ CG 1823 0.358772 12.01 ; qtot -3.85
1824 NA 116 HIQ ND1 1824 -0.372509 14.01 ; qtot -4.056
1825 H 116 HIQ HD1 1825 0.361030 1.008 ; qtot -3.738
1826 CR 116 HIQ CE1 1826 0.020964 12.01 ; qtot -3.591
1827 H5 116 HIQ HE1 1827 0.157317 1.008 ; qtot -3.469
1828 NB 116 HIQ NE2 1828 -0.115046 14.01 ; qtot -4.07
1829 CV 116 HIQ CD2 1829 -0.332913 12.01 ; qtot -4.026
1830 H4 116 HIQ HD2 1830 0.178074 1.008 ; qtot -3.916
1831 C 116 HIQ C 1831 0.515947 12.01 ; qtot -3.4
1832 O 116 HIQ O 1832 -0.599831 16 ; qtot -4

; residue 235 HIX rtp HIX q 0.0
3655 N 235 HIX N 3655 -0.506799 14.01 ; qtot -10.51
3656 H 235 HIX H 3656 0.351021 1.008 ; qtot -10.16
3657 CT 235 HIX CA 3657 0.119066 12.01 ; qtot -10.04
3658 H1 235 HIX HA 3658 0.137761 1.008 ; qtot -9.899
3659 CT 235 HIX CB 3659 -0.122638 12.01 ; qtot -10.02
3660 HC 235 HIX HB1 3660 0.086329 1.008 ; qtot -9.935
3661 HC 235 HIX HB2 3661 0.086329 1.008 ; qtot -9.849
3662 CC 235 HIX CG 3662 0.362487 12.01 ; qtot -9.85
3663 NA 235 HIX ND1 3663 -0.401630 14.01 ; qtot -10.06
3664 H 235 HIX HD1 3664 0.354126 1.008 ; qtot -9.738
3665 CR 235 HIX CE1 3665 0.006603 12.01 ; qtot -9.591
3666 H5 235 HIX HE1 3666 0.146663 1.008 ; qtot -9.469
3667 NB 235 HIX NE2 3667 -0.098290 14.01 ; qtot -10.07
3668 CV 235 HIX CD2 3668 -0.366903 12.01 ; qtot -10.03
3669 H4 235 HIX HD2 3669 0.230197 1.008 ; qtot -9.916
3670 C 235 HIX C 3670 0.515947 12.01 ; qtot -9.4
3671 O 235 HIX O 3671 -0.599831 16 ; qtot -10

```

Substrate-D3

```

; id at type res nr residu name at name cg nr charge
1 FE 1 FER IRO 1 1.000264
2 O 1 FER FEO 1 -0.50310004

; id at type res nr residu name at name cg nr charge
1 Cl 1 CLO CLO 1 -0.575058

; nr type resi res atom cgnr charge mass ; qtot
1 o 1 SUC O 1 -0.647829 16.00000 ; qtot -0.246
2 c 1 SUC C 2 0.744445 12.01000 ; qtot 0.110
3 o 1 SUC O1 3 -0.652057 16.00000 ; qtot -0.136
4 c3 1 SUC C1 4 -0.113137 12.01000 ; qtot -0.077
5 c3 1 SUC C2 5 -0.037569 12.01000 ; qtot -0.017
6 c 1 SUC C3 6 0.855608 12.01000 ; qtot 0.339
7 o 1 SUC O2 7 -0.837781 16.00000 ; qtot 0.093
8 o 1 SUC O3 8 -0.878422 16.00000 ; qtot -0.154
9 hc 1 SUC H 9 0.000406 1.00800 ; qtot -0.115
10 hc 1 SUC H1 10 -0.008403 1.00800 ; qtot -0.077

```

11	hc	1	SUC	H2	11	0.032984	1.00800 ; qtot -0.038
12	hc	1	SUC	H3	12	0.053375	1.00800 ; qtot -0.000

; residue 116 HIQ rtp HIQ q 0.0

1816		N	116	HIQ		N	1816	-0.506799	14.01 ; qtot -4.507
1817		H	116	HIQ		H	1817	0.351021	1.008 ; qtot -4.156
1818		CT	116	HIQ		CA	1818	0.119066	12.01 ; qtot -4.037
1819		H1	116	HIQ		HA	1819	0.137761	1.008 ; qtot -3.899
1820		CT	116	HIQ		CB	1820	-0.122638	12.01 ; qtot -4.022
1821		HC	116	HIQ		HB1	1821	0.086329	1.008 ; qtot -3.935
1822		HC	116	HIQ		HB2	1822	0.086329	1.008 ; qtot -3.849
1823		CC	116	HIQ		CG	1823	0.442784	12.01 ; qtot -3.85
1824		NA	116	HIQ		ND1	1824	-0.444119	14.01 ; qtot -4.056
1825		H	116	HIQ		HD1	1825	0.368646	1.008 ; qtot -3.738
1826		CR	116	HIQ		CE1	1826	0.053689	12.01 ; qtot -3.591
1827		H5	116	HIQ		HE1	1827	0.155198	1.008 ; qtot -3.469
1828		NB	116	HIQ		NE2	1828	-0.112765	14.01 ; qtot -4.07
1829		CV	116	HIQ		CD2	1829	-0.449950	12.01 ; qtot -4.026
1830		H4	116	HIQ		HD2	1830	0.194227	1.008 ; qtot -3.916
1831		C	116	HIQ		C	1831	0.515947	12.01 ; qtot -3.4
1832		O	116	HIQ		O	1832	-0.599831	16 ; qtot -4

; residue 235 HIX rtp HIX q 0.0

3655		N	235	HIX		N	3655	-0.506799	14.01 ; qtot -10.51
3656		H	235	HIX		H	3656	0.351021	1.008 ; qtot -10.16
3657		CT	235	HIX		CA	3657	0.119066	12.01 ; qtot -10.04
3658		H1	235	HIX		HA	3658	0.137761	1.008 ; qtot -9.899
3659		CT	235	HIX		CB	3659	-0.122638	12.01 ; qtot -10.02
3660		HC	235	HIX		HB1	3660	0.086329	1.008 ; qtot -9.935
3661		HC	235	HIX		HB2	3661	0.086329	1.008 ; qtot -9.849
3662		CC	235	HIX		CG	3662	0.308498	12.01 ; qtot -9.85
3663		NA	235	HIX		ND1	3663	-0.302183	14.01 ; qtot -10.06
3664		H	235	HIX		HD1	3664	0.343071	1.008 ; qtot -9.738
3665		CR	235	HIX		CE1	3665	-0.102242	12.01 ; qtot -9.591
3666		H5	235	HIX		HE1	3666	0.171566	1.008 ; qtot -9.469
3667		NB	235	HIX		NE2	3667	-0.016128	14.01 ; qtot -10.07
3668		CV	235	HIX		CD2	3668	-0.351546	12.01 ; qtot -10.03
3669		H4	235	HIX		HD2	3669	0.173122	1.008 ; qtot -9.916
3670		C	235	HIX		C	3670	0.515947	12.01 ; qtot -9.4
3671		O	235	HIX		O	3671	-0.599831	16 ; qtot -10

Substrate-D4

; id at type		res nr	residu name	at name	cg nr	charge	
1	FE	1	FER	IRO	1	1.034717	
2	0	1	FER	FEO	1	-0.574945	
; id at type		res nr	residu name	at name	cg nr	charge	
1	C1	1	CLO	CL0	1	-0.550890	
; nr type resi res atom cgnr charge mass ; qtot							
1	o	1	SUC	O	1	-0.669822	16.00000 ; qtot -0.246
2	c	1	SUC	C	2	0.764680	12.01000 ; qtot 0.110
3	o	1	SUC	O1	3	-0.659302	16.00000 ; qtot -0.136
4	c3	1	SUC	C1	4	-0.125507	12.01000 ; qtot -0.077
5	c3	1	SUC	C2	5	-0.002997	12.01000 ; qtot -0.017
6	c	1	SUC	C3	6	0.854765	12.01000 ; qtot 0.339
7	o	1	SUC	O2	7	-0.874124	16.00000 ; qtot 0.093
8	o	1	SUC	O3	8	-0.846563	16.00000 ; qtot -0.154
9	hc	1	SUC	H	9	-0.019375	1.00800 ; qtot -0.115
10	hc	1	SUC	H1	10	-0.013920	1.00800 ; qtot -0.077
11	hc	1	SUC	H2	11	0.059759	1.00800 ; qtot -0.038

12 hc 1 SUC H3 12 0.030117 1.00800 ; qtot -0.000

; residue 116 HIQ rtp HIQ q 0.0

1816	N	116	HIQ	N	1816	-0.506799	14.01	;	qtot -4.507
1817	H	116	HIQ	H	1817	0.351021	1.008	;	qtot -4.156
1818	CT	116	HIQ	CA	1818	0.119066	12.01	;	qtot -4.037
1819	H1	116	HIQ	HA	1819	0.137761	1.008	;	qtot -3.899
1820	CT	116	HIQ	CB	1820	-0.122638	12.01	;	qtot -4.022
1821	HC	116	HIQ	HB1	1821	0.086329	1.008	;	qtot -3.935
1822	HC	116	HIQ	HB2	1822	0.086329	1.008	;	qtot -3.849
1823	CC	116	HIQ	CG	1823	0.392287	12.01	;	qtot -3.85
1824	NA	116	HIQ	ND1	1824	-0.365249	14.01	;	qtot -4.056
1825	H	116	HIQ	HD1	1825	0.353521	1.008	;	qtot -3.738
1826	CR	116	HIQ	CE1	1826	-0.036499	12.01	;	qtot -3.591
1827	H5	116	HIQ	HE1	1827	0.183276	1.008	;	qtot -3.469
1828	NB	116	HIQ	NE2	1828	-0.078236	14.01	;	qtot -4.07
1829	CV	116	HIQ	CD2	1829	-0.440544	12.01	;	qtot -4.026
1830	H4	116	HIQ	HD2	1830	0.196387	1.008	;	qtot -3.916
1831	C	116	HIQ	C	1831	0.515947	12.01	;	qtot -3.4
1832	O	116	HIQ	O	1832	-0.599831	16	;	qtot -4

; residue 235 HIX rtp HIX q 0.0

3655	N	235	HIX	N	3655	-0.506799	14.01	;	qtot -10.51
3656	H	235	HIX	H	3656	0.351021	1.008	;	qtot -10.16
3657	CT	235	HIX	CA	3657	0.119066	12.01	;	qtot -10.04
3658	H1	235	HIX	HA	3658	0.137761	1.008	;	qtot -9.899
3659	CT	235	HIX	CB	3659	-0.122638	12.01	;	qtot -10.02
3660	HC	235	HIX	HB1	3660	0.086329	1.008	;	qtot -9.935
3661	HC	235	HIX	HB2	3661	0.086329	1.008	;	qtot -9.849
3662	CC	235	HIX	CG	3662	0.369485	12.01	;	qtot -9.85
3663	NA	235	HIX	ND1	3663	-0.348861	14.01	;	qtot -10.06
3664	H	235	HIX	HD1	3664	0.351716	1.008	;	qtot -9.738
3665	CR	235	HIX	CE1	3665	-0.066350	12.01	;	qtot -9.591
3666	H5	235	HIX	HE1	3666	0.172700	1.008	;	qtot -9.469
3667	NB	235	HIX	NE2	3667	0.008000	14.01	;	qtot -10.07
3668	CV	235	HIX	CD2	3668	-0.446081	12.01	;	qtot -10.03
3669	H4	235	HIX	HD2	3669	0.213484	1.008	;	qtot -9.916
3670	C	235	HIX	C	3670	0.515947	12.01	;	qtot -9.4
3671	O	235	HIX	O	3671	-0.599831	16	;	qtot -10

Substrate-D4

; id at type res nr residu name at name cg nr charge

1	FE		1	FER		IRO	1	0.793927	
2	0		1	FER		FEO	1	-0.578432	

; id at type res nr residu name at name cg nr charge

1	C1		1	CLO		CLO	1	-0.500775	

; nr type resi res atom cgnr charge mass ; qtot

1	o	1	LIG	O	1	-0.709408	16.00000	;	qtot -0.246
2	c	1	LIG	C	2	0.787417	12.01000	;	qtot 0.110
3	o	1	LIG	O1	3	-0.515985	16.00000	;	qtot -0.136
4	c3	1	LIG	C1	4	-0.309409	12.01000	;	qtot -0.077
5	c3	1	LIG	C2	5	0.156446	12.01000	;	qtot -0.017
6	c	1	LIG	C3	6	0.748318	12.01000	;	qtot 0.339
7	o	1	LIG	O2	7	-0.852347	16.00000	;	qtot 0.093
8	o	1	LIG	O3	8	-0.807292	16.00000	;	qtot -0.154
9	hc	1	LIG	H	9	-0.031508	1.00800	;	qtot -0.115
10	hc	1	LIG	H1	10	-0.067819	1.00800	;	qtot -0.077
11	hc	1	LIG	H2	11	0.063750	1.00800	;	qtot -0.038
12	hc	1	LIG	H3	12	0.059706	1.00800	;	qtot -0.000

```
; residue 116 HIQ rtp HIQ q 0.0
 1816      N   116    HIQ      N   1816 -0.506799   14.01 ; qtot -4.507
 1817      H   116    HIQ      H   1817  0.351021   1.008 ; qtot -4.156
 1818     CT   116    HIQ     CA  1818  0.119066  12.01 ; qtot -4.037
 1819      H1   116    HIQ     HA  1819  0.137761  1.008 ; qtot -3.899
 1820     CT   116    HIQ     CB  1820 -0.122638  12.01 ; qtot -4.022
 1821     HC   116    HIQ    HB1  1821  0.086329   1.008 ; qtot -3.935
 1822     HC   116    HIQ    HB2  1822  0.086329   1.008 ; qtot -3.849
 1823     CC   116    HIQ     CG  1823  0.339699  12.01 ; qtot -3.85
 1824     NA   116    HIQ    ND1  1824 -0.312577  14.01 ; qtot -4.056
 1825      H   116    HIQ    HD1  1825  0.338124   1.008 ; qtot -3.738
 1826     CR   116    HIQ    CE1  1826 -0.090369  12.01 ; qtot -3.591
 1827     H5   116    HIQ    HE1  1827  0.179567   1.008 ; qtot -3.469
 1828     NB   116    HIQ    NE2  1828 -0.116037  14.01 ; qtot -4.07
 1829     CV   116    HIQ    CD2  1829 -0.266276  12.01 ; qtot -4.026
 1830     H4   116    HIQ    HD2  1830  0.193220   1.008 ; qtot -3.916
 1831      C   116    HIQ      C  1831  0.515947  12.01 ; qtot -3.4
 1832      O   116    HIQ      O  1832 -0.599831   16 ; qtot -4
```

```
; residue 235 HIX rtp HIX q 0.0
 3655      N   235    HIX      N  3655 -0.506799   14.01 ; qtot -10.51
 3656      H   235    HIX      H  3656  0.351021   1.008 ; qtot -10.16
 3657     CT   235    HIX     CA  3657  0.119066  12.01 ; qtot -10.04
 3658     H1   235    HIX     HA  3658  0.137761   1.008 ; qtot -9.899
 3659     CT   235    HIX     CB  3659 -0.122638  12.01 ; qtot -10.02
 3660     HC   235    HIX    HB1  3660  0.086329   1.008 ; qtot -9.935
 3661     HC   235    HIX    HB2  3661  0.086329   1.008 ; qtot -9.849
 3662     CC   235    HIX     CG  3662  0.358329  12.01 ; qtot -9.85
 3663     NA   235    HIX    ND1  3663 -0.324563  14.01 ; qtot -10.06
 3664      H   235    HIX    HD1  3664  0.343920   1.008 ; qtot -9.738
 3665     CR   235    HIX    CE1  3665 -0.145887  12.01 ; qtot -9.591
 3666     H5   235    HIX    HE1  3666  0.192682   1.008 ; qtot -9.469
 3667     NB   235    HIX    NE2  3667  0.139527  14.01 ; qtot -10.07
 3668     CV   235    HIX    CD2  3668 -0.474968  12.01 ; qtot -10.03
 3669     H4   235    HIX    HD2  3669  0.274650   1.008 ; qtot -9.916
 3670      C   235    HIX      C  3670  0.515947  12.01 ; qtot -9.4
 3671      O   235    HIX      O  3671 -0.599831   16 ; qtot -10
```

THR

	nr	type	resi	res	atom	cgnr	charge	mass		; qtot	bond_type
;											
1	c3	1	LIG	C	1	0.028003	12.01000	;	qtot	0.028	
2	os	1	LIG	O	2	-0.185718	16.00000	;	qtot	-0.158	
3	c3	1	LIG	C	3	-0.317708	12.01000	;	qtot	-0.475	
4	c3	1	LIG	C	4	0.411177	12.01000	;	qtot	-0.064	
5	c3	1	LIG	C	5	-0.404402	12.01000	;	qtot	-0.469	
6	c3	1	LIG	C	6	-0.289491	12.01000	;	qtot	-0.758	
7	c3	1	LIG	C	7	-0.195934	12.01000	;	qtot	-0.954	
8	oh	1	LIG	O	8	-0.580049	16.00000	;	qtot	-1.534	
9	ho	1	LIG	H	9	0.396549	1.00800	;	qtot	-1.138	
10	c	1	LIG	C	10	0.704642	12.01000	;	qtot	-0.433	
11	o	1	LIG	O	11	-0.621570	16.00000	;	qtot	-1.055	
12	n	1	LIG	N	12	-0.498288	14.01000	;	qtot	-1.553	
13	hn	1	LIG	H	13	0.323545	1.00800	;	qtot	-1.229	
14	c3	1	LIG	C	14	0.332134	12.01000	;	qtot	-0.897	
15	c3	1	LIG	C	15	-0.540514	12.01000	;	qtot	-1.438	
16	c	1	LIG	C	16	0.726795	12.01000	;	qtot	-0.711	
17	n	1	LIG	N	17	-0.718367	14.01000	;	qtot	-1.429	
18	hn	1	LIG	H	18	0.459514	1.00800	;	qtot	-0.970	
19	o	1	LIG	O	19	-0.546523	16.00000	;	qtot	-1.516	
20	c3	1	LIG	C	20	0.064949	12.01000	;	qtot	-1.451	

21	c3	1	LIG	C	21	0.116089	12.01000 ; qtot -1.335
22	ss	1	LIG	S	22	-0.220764	32.06000 ; qtot -1.556
23	c	1	LIG	C	23	0.283013	12.01000 ; qtot -1.273
24	o	1	LIG	O	24	-0.286551	16.00000 ; qtot -1.559
25	c3	1	LIG	C	25	-0.199664	12.01000 ; qtot -1.759
26	n4	1	LIG	N	26	-0.379375	14.01000 ; qtot -2.139
27	hn	1	LIG	H	27	0.326271	1.00800 ; qtot -1.812
28	hn	1	LIG	H	28	0.348370	1.00800 ; qtot -1.464
29	hn	1	LIG	H	29	0.353612	1.00800 ; qtot -1.110
30	c3	1	LIG	C	30	0.256880	12.01000 ; qtot -0.853
31	c3	1	LIG	C	31	-0.545099	12.01000 ; qtot -1.398
32	oh	1	LIG	O	32	-0.623469	16.00000 ; qtot -2.022
33	ho	1	LIG	H	33	0.458110	1.00800 ; qtot -1.564
34	h1	1	LIG	H	34	0.023394	1.00800 ; qtot -1.540
35	h1	1	LIG	H	35	0.035041	1.00800 ; qtot -1.505
36	h1	1	LIG	H	36	0.160190	1.00800 ; qtot -1.345
37	h1	1	LIG	H	37	0.121151	1.00800 ; qtot -1.224
38	h1	1	LIG	H	38	0.117080	1.00800 ; qtot -1.107
39	hc	1	LIG	H	39	0.123884	1.00800 ; qtot -0.983
40	hc	1	LIG	H	40	0.092629	1.00800 ; qtot -0.890
41	hc	1	LIG	H	41	0.089118	1.00800 ; qtot -0.801
42	hc	1	LIG	H	42	0.057960	1.00800 ; qtot -0.743
43	hc	1	LIG	H	43	0.041257	1.00800 ; qtot -0.702
44	hc	1	LIG	H	44	0.077798	1.00800 ; qtot -0.624
45	h1	1	LIG	H	45	0.100299	1.00800 ; qtot -0.524
46	h1	1	LIG	H	46	-0.020691	1.00800 ; qtot -0.545
47	h1	1	LIG	H	47	0.026070	1.00800 ; qtot -0.519
48	hc	1	LIG	H	48	0.151272	1.00800 ; qtot -0.367
49	hc	1	LIG	H	49	0.164587	1.00800 ; qtot -0.203
50	h1	1	LIG	H	50	0.093264	1.00800 ; qtot -0.110
51	h1	1	LIG	H	51	0.079883	1.00800 ; qtot -0.030
52	h1	1	LIG	H	52	0.100083	1.00800 ; qtot 0.070
53	h1	1	LIG	H	53	0.078269	1.00800 ; qtot 0.149
54	hx	1	LIG	H	54	0.220092	1.00800 ; qtot 0.369
55	h1	1	LIG	H	55	0.121156	1.00800 ; qtot 0.490
56	hc	1	LIG	H	56	0.168836	1.00800 ; qtot 0.659
57	hc	1	LIG	H	57	0.191533	1.00800 ; qtot 0.850
58	hc	1	LIG	H	58	0.149672	1.00800 ; qtot 1.000

ABA

;	nr	type	resi	res	atom	cgnr	charge	mass ; qtot bond_type
1	c	1	LIG	C	1	0.563045	12.01000 ; qtot 0.563	
2	n	1	LIG	N	2	-0.541920	14.01000 ; qtot 0.021	
3	hn	1	LIG	H	3	0.367593	1.00800 ; qtot 0.389	
4	o	1	LIG	O	4	-0.527199	16.00000 ; qtot -0.138	
5	c3	1	LIG	C1	5	-0.219109	12.01000 ; qtot -0.358	
6	c3	1	LIG	C2	6	0.100436	12.01000 ; qtot -0.257	
7	n	1	LIG	N1	7	-0.315634	14.01000 ; qtot -0.573	
8	hn	1	LIG	H1	8	0.225383	1.00800 ; qtot -0.347	
9	c	1	LIG	C3	9	0.681581	12.01000 ; qtot 0.334	
10	o	1	LIG	O1	10	-0.667566	16.00000 ; qtot -0.333	
11	c3	1	LIG	C4	11	-0.161290	12.01000 ; qtot -0.495	
12	c3	1	LIG	C5	12	0.424332	12.01000 ; qtot -0.070	
13	c3	1	LIG	C6	13	-0.309853	12.01000 ; qtot -0.380	
14	c3	1	LIG	C7	14	-0.320006	12.01000 ; qtot -0.700	
15	c3	1	LIG	C8	15	0.031176	12.01000 ; qtot -0.669	
16	os	1	LIG	O2	16	-0.271069	16.00000 ; qtot -0.940	
17	c3	1	LIG	C9	17	-0.194687	12.01000 ; qtot -1.135	
18	oh	1	LIG	O3	18	-0.610788	16.00000 ; qtot -1.746	
19	ho	1	LIG	H2	19	0.412076	1.00800 ; qtot -1.333	
20	c3	1	LIG	C10	20	0.017000	12.01000 ; qtot -1.316	

21	c3	1	LIG	C11	21	0.013460	12.01000 ; qtot -1.303
22	ss	1	LIG	S	22	-0.141459	32.06000 ; qtot -1.444
23	c	1	LIG	C12	23	0.236091	12.01000 ; qtot -1.208
24	o	1	LIG	O4	24	-0.363981	16.00000 ; qtot -1.572
25	c3	1	LIG	C13	25	0.122405	12.01000 ; qtot -1.450
26	n4	1	LIG	N2	26	-0.439849	14.01000 ; qtot -1.890
27	hn	1	LIG	H3	27	0.356848	1.00800 ; qtot -1.533
28	hn	1	LIG	H4	28	0.381851	1.00800 ; qtot -1.151
29	hn	1	LIG	H5	29	0.334026	1.00800 ; qtot -0.817
30	c3	1	LIG	C14	30	0.179588	12.01000 ; qtot -0.638
31	c3	1	LIG	C15	31	-0.303564	12.01000 ; qtot -0.941
32	hc	1	LIG	H6	32	0.089303	1.00800 ; qtot -0.852
33	hc	1	LIG	H7	33	0.084175	1.00800 ; qtot -0.768
34	h1	1	LIG	H8	34	0.063493	1.00800 ; qtot -0.704
35	h1	1	LIG	H9	35	0.031689	1.00800 ; qtot -0.672
36	h1	1	LIG	H10	36	0.086124	1.00800 ; qtot -0.586
37	hc	1	LIG	H11	37	0.055773	1.00800 ; qtot -0.531
38	hc	1	LIG	H12	38	0.075055	1.00800 ; qtot -0.455
39	hc	1	LIG	H13	39	0.058690	1.00800 ; qtot -0.397
40	hc	1	LIG	H14	40	0.061600	1.00800 ; qtot -0.335
41	hc	1	LIG	H15	41	0.073139	1.00800 ; qtot -0.262
42	hc	1	LIG	H16	42	0.064882	1.00800 ; qtot -0.197
43	h1	1	LIG	H17	43	0.046192	1.00800 ; qtot -0.151
44	h1	1	LIG	H18	44	0.045894	1.00800 ; qtot -0.105
45	h1	1	LIG	H19	45	0.123584	1.00800 ; qtot 0.019
46	h1	1	LIG	H20	46	0.093463	1.00800 ; qtot 0.112
47	h1	1	LIG	H21	47	0.091840	1.00800 ; qtot 0.204
48	h1	1	LIG	H22	48	0.092664	1.00800 ; qtot 0.296
49	h1	1	LIG	H23	49	0.092444	1.00800 ; qtot 0.389
50	h1	1	LIG	H24	50	0.130940	1.00800 ; qtot 0.520
51	h1	1	LIG	H25	51	0.077285	1.00800 ; qtot 0.597
52	hx	1	LIG	H26	52	0.112270	1.00800 ; qtot 0.709
53	hc	1	LIG	H27	53	0.022432	1.00800 ; qtot 0.732
54	hc	1	LIG	H28	54	-0.004045	1.00800 ; qtot 0.728
55	hc	1	LIG	H29	55	0.079242	1.00800 ; qtot 0.807
56	hc	1	LIG	H30	56	0.084802	1.00800 ; qtot 0.892
57	hc	1	LIG	H31	57	0.108150	1.00800 ; qtot 1.000

NVA

;	nr	type	resi	res	atom	cgnr	charge	mass ; qtot bond_type
1	c	1	LIG	C	1	0.594353	12.01000 ; qtot 0.594	
2	n	1	LIG	N	2	-0.642777	14.01000 ; qtot -0.048	
3	hn	1	LIG	H	3	0.377152	1.00800 ; qtot 0.329	
4	o	1	LIG	O	4	-0.533358	16.00000 ; qtot -0.205	
5	c3	1	LIG	C1	5	-0.221485	12.01000 ; qtot -0.426	
6	c3	1	LIG	C2	6	0.076077	12.01000 ; qtot -0.350	
7	n	1	LIG	N1	7	-0.353068	14.01000 ; qtot -0.703	
8	hn	1	LIG	H1	8	0.245176	1.00800 ; qtot -0.458	
9	c	1	LIG	C3	9	0.689601	12.01000 ; qtot 0.232	
10	o	1	LIG	O1	10	-0.664014	16.00000 ; qtot -0.432	
11	c3	1	LIG	C4	11	-0.160891	12.01000 ; qtot -0.593	
12	c3	1	LIG	C5	12	0.363843	12.01000 ; qtot -0.229	
13	c3	1	LIG	C6	13	-0.351007	12.01000 ; qtot -0.580	
14	c3	1	LIG	C7	14	-0.345587	12.01000 ; qtot -0.926	
15	c3	1	LIG	C8	15	0.143370	12.01000 ; qtot -0.783	
16	os	1	LIG	O2	16	-0.289542	16.00000 ; qtot -1.072	
17	c3	1	LIG	C9	17	-0.208274	12.01000 ; qtot -1.280	
18	oh	1	LIG	O3	18	-0.603889	16.00000 ; qtot -1.884	
19	ho	1	LIG	H2	19	0.406190	1.00800 ; qtot -1.478	
20	c3	1	LIG	C10	20	0.229184	12.01000 ; qtot -1.249	
21	c3	1	LIG	C11	21	-0.019238	12.01000 ; qtot -1.268	

22	ss	1	LIG	S	22	-0.149641	32.06000 ; qtot -1.418
23	c	1	LIG	C12	23	0.314334	12.01000 ; qtot -1.103
24	o	1	LIG	O4	24	-0.387219	16.00000 ; qtot -1.491
25	c3	1	LIG	C13	25	0.021667	12.01000 ; qtot -1.469
26	n4	1	LIG	N2	26	-0.534559	14.01000 ; qtot -2.004
27	hn	1	LIG	H3	27	0.375569	1.00800 ; qtot -1.628
28	hn	1	LIG	H4	28	0.412932	1.00800 ; qtot -1.215
29	hn	1	LIG	H5	29	0.373633	1.00800 ; qtot -0.841
30	c3	1	LIG	C14	30	-0.032791	12.01000 ; qtot -0.874
31	c3	1	LIG	C15	31	0.303287	12.01000 ; qtot -0.571
32	c3	1	LIG	C16	32	-0.372728	12.01000 ; qtot -0.944
33	hc	1	LIG	H6	33	0.095783	1.00800 ; qtot -0.848
34	hc	1	LIG	H7	34	0.088785	1.00800 ; qtot -0.759
35	h1	1	LIG	H8	35	0.073853	1.00800 ; qtot -0.685
36	h1	1	LIG	H9	36	0.040517	1.00800 ; qtot -0.645
37	h1	1	LIG	H10	37	0.095754	1.00800 ; qtot -0.549
38	hc	1	LIG	H11	38	0.069619	1.00800 ; qtot -0.479
39	hc	1	LIG	H12	39	0.085855	1.00800 ; qtot -0.394
40	hc	1	LIG	H13	40	0.079225	1.00800 ; qtot -0.314
41	hc	1	LIG	H14	41	0.067648	1.00800 ; qtot -0.247
42	hc	1	LIG	H15	42	0.090665	1.00800 ; qtot -0.156
43	hc	1	LIG	H16	43	0.071043	1.00800 ; qtot -0.085
44	h1	1	LIG	H17	44	0.026701	1.00800 ; qtot -0.058
45	h1	1	LIG	H18	45	0.020637	1.00800 ; qtot -0.038
46	h1	1	LIG	H19	46	0.129349	1.00800 ; qtot 0.092
47	h1	1	LIG	H20	47	0.095040	1.00800 ; qtot 0.187
48	h1	1	LIG	H21	48	0.092330	1.00800 ; qtot 0.279
49	h1	1	LIG	H22	49	0.037340	1.00800 ; qtot 0.316
50	h1	1	LIG	H23	50	0.050219	1.00800 ; qtot 0.367
51	h1	1	LIG	H24	51	0.128813	1.00800 ; qtot 0.495
52	h1	1	LIG	H25	52	0.072863	1.00800 ; qtot 0.568
53	hx	1	LIG	H26	53	0.145235	1.00800 ; qtot 0.714
54	hc	1	LIG	H27	54	0.017256	1.00800 ; qtot 0.731
55	hc	1	LIG	H28	55	0.065916	1.00800 ; qtot 0.797
56	hc	1	LIG	H29	56	-0.036007	1.00800 ; qtot 0.761
57	hc	1	LIG	H30	57	-0.036148	1.00800 ; qtot 0.725
58	hc	1	LIG	H31	58	0.091636	1.00800 ; qtot 0.816
59	hc	1	LIG	H32	59	0.098584	1.00800 ; qtot 0.915
60	hc	1	LIG	H33	60	0.085185	1.00800 ; qtot 1.000

1.4 QM/MM setup

For the purposes of the microiterative QM/MM optimisations¹⁸, the system is divided into an inner region, which is updated less frequently, and an outer region, which is optimised to convergence for every step taken in the inner region. The inner region comprised all residues with at least one QM atom (106 atoms for **THR**). Only atoms in the active region are allowed to move in optimisations; the active region included all residues within 8 Å of any atom in the inner region (1550 atoms for **THR**). The HDLC residues used for optimisations coincided with the standard amino-acid residues of the protein; non-standard components (substrate, active-site iron complex) were grouped into chemically meaningful HDLC residues (substrate, [FeCl(2OG)(O₂)]).

The reaction coordinate was implemented by a harmonic restraint with a force constant of 3.0 $E_h a_0^{-2}$.

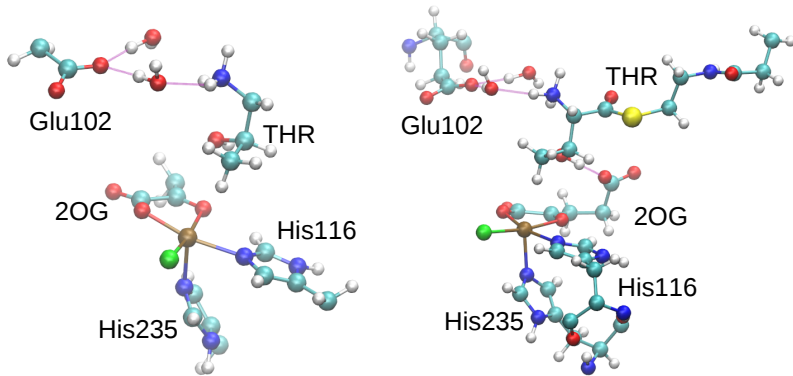


Figure S1: Partitioning of the system for QM/MM calculations and microiterative optimisations (illustrated for **THR**). Left: QM region (without link atoms). Right: Inner region for microiterative optimisations.

2 Supplementary Results

2.1 Docking

Table S3: The ten docked poses of NVA with highest affinity

Pose	Affinity (kJ/mol)	RMSD (Å)
1	-31.8	0.00
2	-31.4	1.69
3	-31.0	1.86
4	-30.1	2.26
5	-28.9	2.06
6	-28.5	9.75
7	-28.0	9.60
8	-28.0	5.46
9	-28.0	9.43
10	-28.0	7.86

Table S4: The ten docked poses of ABA with highest affinity

Pose	Affinity (kJ/mol)	RMSD (Å)
1	-32.6	0.00
2	-32.2	1.88
3	-31.4	2.08
4	-30.1	2.44
5	-29.7	9.33
6	-29.3	5.19
7	-29.3	9.51
8	-29.3	9.59
9	-29.3	9.67
10	-29.3	9.704

2.2 MD simulations

2.2.1 Simulations of the apoprotein, holoprotein, and substrate-A complexes

In addition to the three substrate–A complexes, the holoprotein (**A-H₂O**, containing the active-site iron complex with ZOG, Cl, and H₂O ligands, but no substrate) and the apoprotein (i.e., the “bare” protein) were also simulated using the same protocol. In all cases, the equilibrated structures remained very close to the crystal structure of the holoprotein (PDB code 2FCT): the RMSDs (calculated for backbone atoms, averaged over the equilibrated section of the trajectory) were 1.24 Å (apoprotein), 1.15 Å (holoprotein), 1.95 Å (**THR-A**), 1.33 Å (**ABA-A**), 1.24 Å (**NVA-A**).

The conformation of the benzyl side-chain of the “gate-keeper” residue Phe196 is determined by the C–C^α–C^β–C^γ and C^α–C^β–C^γ–C^δ torsions (see Table S5). The side-chain conformations for the three docked structures are nearly identical, with the phenyl ring being positioned such as to allow the substrate access to the active-site channel. In the MD simulations, we find different rotamers for the different systems, including cases where two rotamers are significantly populated (Figure S4). As the protein is fully flexible in the MD simulations, the channel and “gate” on the one hand and the bound substrate on the other are able to adjust their conformations to allow a best (induced) fit; for instance, the Phe196 side-chain adopts the “closed” conformation of the holoprotein in **THR-A**. The “gate” is thus more aptly characterised as a “curtain”, which can flexibly wrap around, and yield to, an obstacle placed in the doorway.

Table S5: Side-chain torsions of the “gate-keeper” residue Phe196; values from docking refer to the top pose, MD values are converged averages.

	Method	C–C ^α –C ^β –C ^γ (°)	C ^α –C ^β –C ^γ –C ^δ (°)
A-H₂O (holoprotein)	X-ray	-167	-77
	MD	-170	-68
THR-A	Docking	135	-31
	MD	175	-70
ABA-A	Docking	134	-35
	MD	68, 156	-50
NVA-A	Docking	133	-33
	MD	75	90

Hydrogen Bonding Partners of the THR OH group

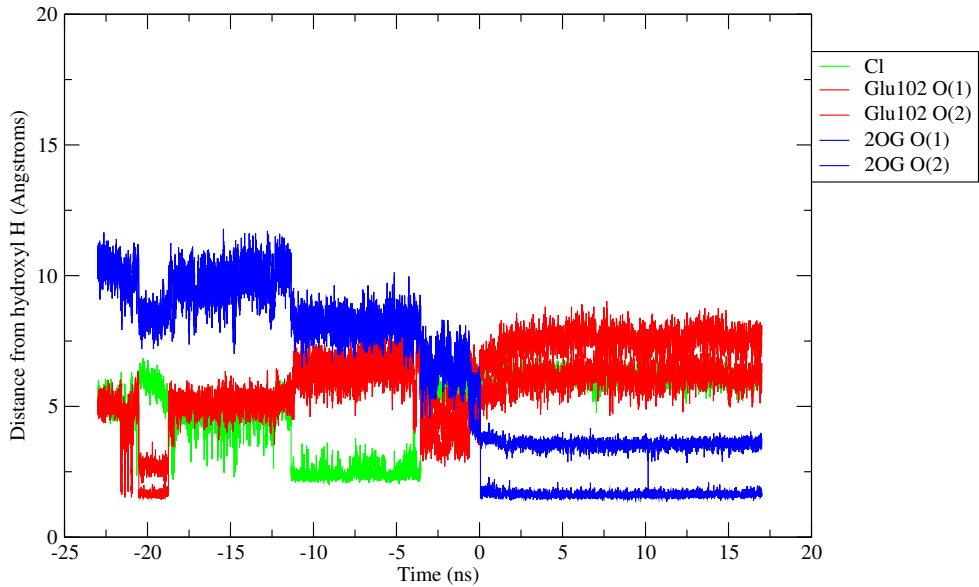


Figure S2: Hydrogen-bonding partners of the **THR-A** OH group over the course of the MD trajectory. Time zero refers to the start of the equilibrated section of the trajectory. 2OG O(1) and O(2) refer to the oxygen atoms of the 2OG tail carboxylate; Glu102 O(1) and O(2) to the carboxylate oxygens of Glu102.

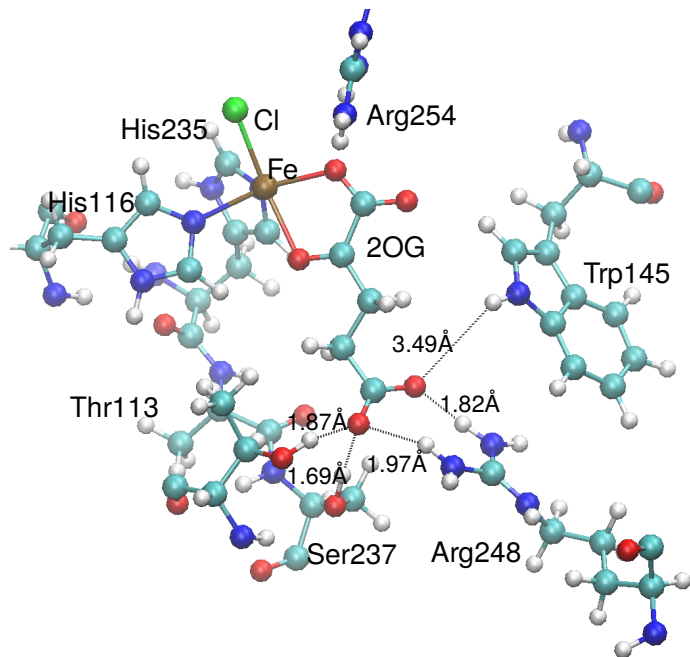


Figure S3: Representative snapshot illustrating the hydrogen-bonding network around the 2OG carboxylate tail as found in the equilibrated structures of **ABA-A** and **NVA-A**.

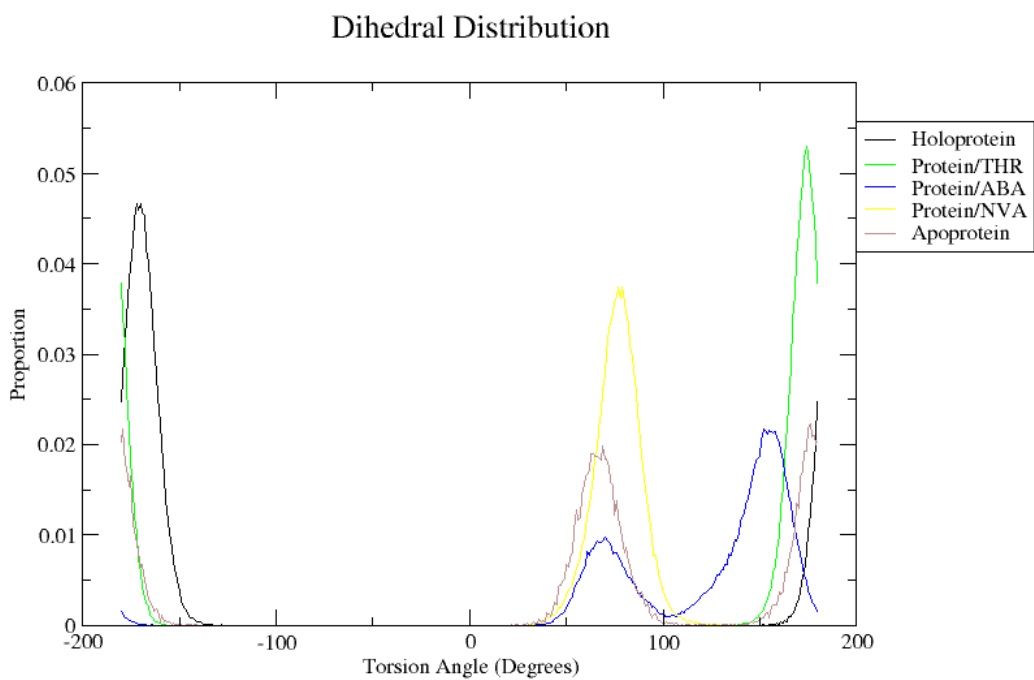


Figure S4: Distribution of the $\text{C}-\text{C}^\alpha-\text{C}^\beta-\text{C}^\gamma$ dihedral angle of Phe196. In the crystal structure of the SyrB2 holoprotein (PDB 2FCT), the value of this torsion is -167° .

2.2.2 Accessibility of the active site for small molecules

Over the course of the catalytic cycle, O₂ is consumed and CO₂ is generated. The crystal structure of the SyrB2 holoprotein features two channels connecting the active-site cavity to the surface: the main substrate channel (T_1) and an allosteric channel (T_2); see Figure S5. Two questions arise as to the accessibility of the active site for small molecules: (i) Do the channels identified in the crystal structure remain intact and open during the course of MD? (ii) Does the bound substrate plug the main channel, leaving only (T_2) as a route for small molecules to access the active-site cavity?

The MD trajectories for the holoprotein and the enzyme–substrate complexes were analysed using the program Caver.¹⁹ Caver searches the trajectory frame-by-frame for tunnels, then groups related tunnels from different frames into channels; a tunnel is represented as an “elastic hose”, whose shape, length, and diameter vary over the course of the trajectory, reflecting the conformational dynamics of the protein. Each channel is assigned an importance (priority) value according to its length, width, and the duration for which it persists. This value is calculated from a cost function (Eq. 1), which depends on overall length L and the varying radius along the tunnel, $r(s)$; long, narrow tunnels have a high cost. The cost may be understood as a measure of the energy required to traverse the tunnel. The priority (Eq. 2) is then calculated from the cost by Boltzmann-weighting and averaging over time (N is the number of frames). The priority value effectively measures the transport capacity of a channel.

$$C = \int_0^L r(s)^{-2} ds \quad (1)$$

$$\text{Priority} = \frac{1}{N} \sum_{i=1}^N e^{-C_i} \quad (2)$$

The results of this analysis are shown in Table S6. No new channels opened during the MD simulations, but both T_1 and T_2 remained open in all simulations, even when the substrate was bound.

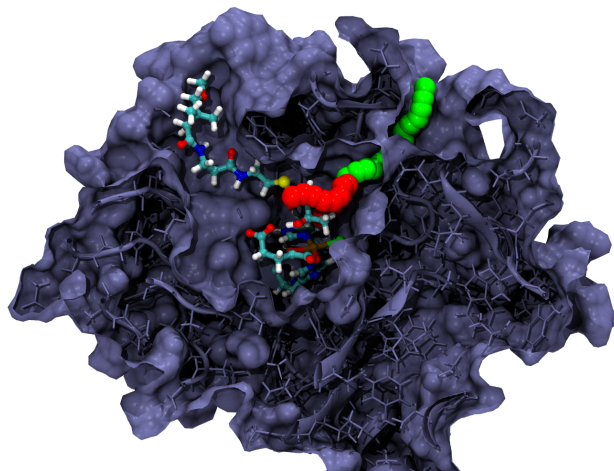


Figure S5: Channels in SyrB2 **THR-A** (T_1 shown in red, T_2 shown in green).

Table S6: Channels leading to active site. r_{\min} is the bottleneck radius, L is the average length. **ABA** yielded two routes through the main channel, above and below the substrate.

Simulation	T_1			T_2		
	Priority	r_{\min} (Å)	L (Å)	Priority	r_{\min} (Å)	L (Å)
Holoprotein	0.192	0.96	21.7	0.081	0.96	23.6
THR	0.280	1.00	16.1	0.203	1.00	22.3
ABA	0.031	0.96	14.8	0.008	0.96	25.1
	0.009	0.93	29.1			
NVA	0.008	0.96	15.7	0.028	0.94	22.7

2.2.3 Simulations of substrate-D complexes

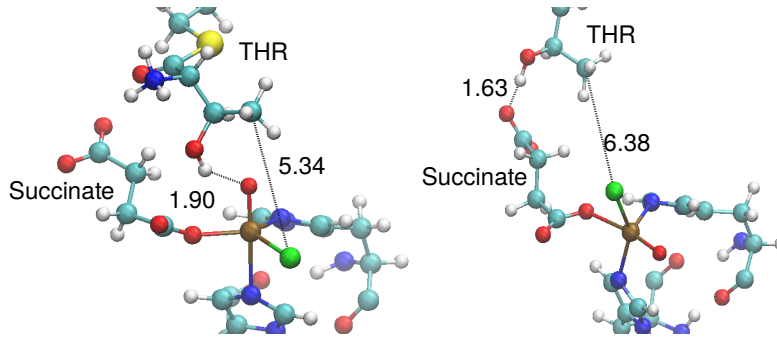


Figure S6: Representative snapshots of **THR-D2** (left) and **THR-D5** (right).

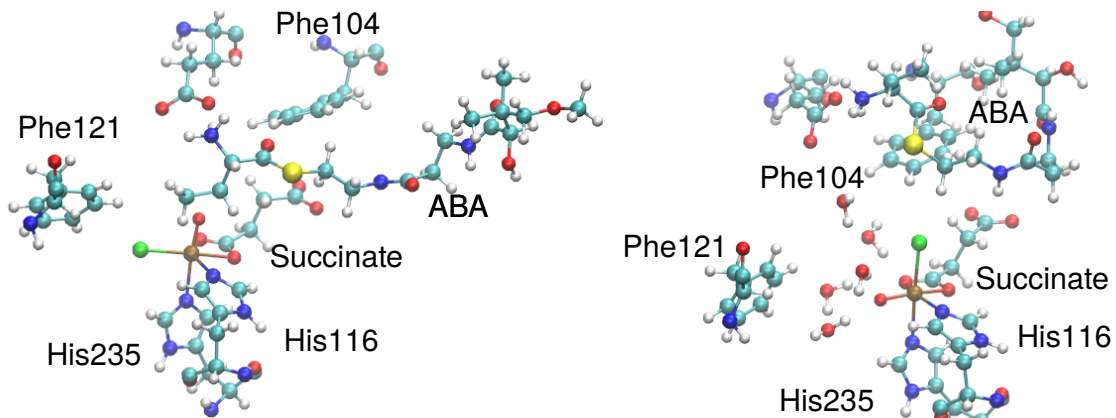


Figure S7: Representative snapshots of **ABA-D3** (left), which adopts a stable conformation, and **ABA-D4** (right), which did not settle into a stable conformation during the simulations.

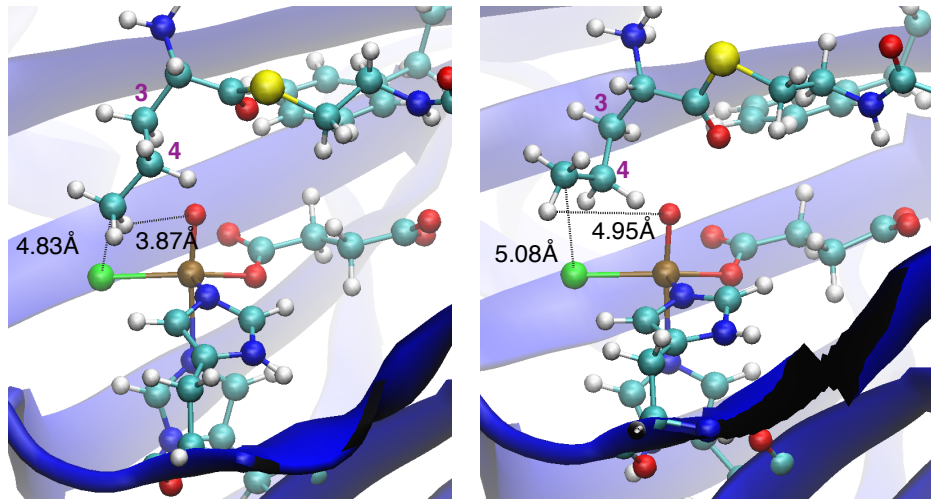


Figure S8: Representative snapshots of **NVA-D2** in the major (left) and minor (right) C³-C⁴ rotamer.

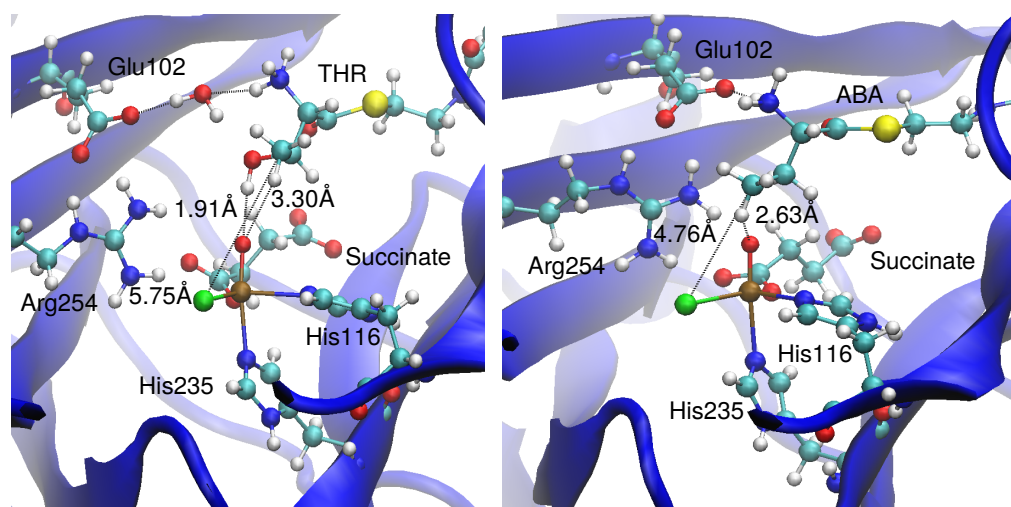


Figure S9: Representative snapshots of **THR-D2** (left) and **ABA-D2** (right). As seen already in the simulations with **B**, **ABA-D** maintains the direct salt bridge between the ammonium group and Glu102 whilst for **THR-D** this salt bridge is indirect, i.e., mediated by a water molecule.

2.2.4 Hydrogen-bond coordination number of the oxido oxygen

In the Mössbauer spectrum of SyrB2 with its native **THR** substrate, two distinct [Fe=O] species are observed²⁰. This was explained by Wong *et al.*²¹ by different numbers of hydrogen bonds to the oxido ligand, rather than by geometrical isomerism²². We therefore analysed the trajectories with the isomers **D1** and **D2** with respect to the hydrogen-bond coordination numbers of the oxido ligand (see Table S7). If we presume that the two species differ by one hydrogen bond, none of the ratios for **THR** (1 vs. 0 and 2 vs. 1 H-bonds, respectively) matches particularly well with the experimental ratio between the two [Fe=O] species of 4:1. For **ABA**, the experimental ratio is 7:1, which agrees nicely with the ratio of 8:1 for 0 vs. 1 H-bond in **ABA-D2**. However, based on these limited data, we can neither support nor reject Wong *et al.*'s proposal.

Table S7: Prevalence of hydrogen-bond coordination numbers to oxido.

Substrate	Isomer	% of frames with n H-bonds to oxido		
		$n = 0$	$n = 1$	$n = 2$
THR	D1	38	55	7
	D2	26	68	6
ABA	D1	33	52	14
	D2	88	11	0
NVA	D1	26	68	6
	D2	33	52	14

2.3 QM/MM calculations

2.3.1 O₂ complexes

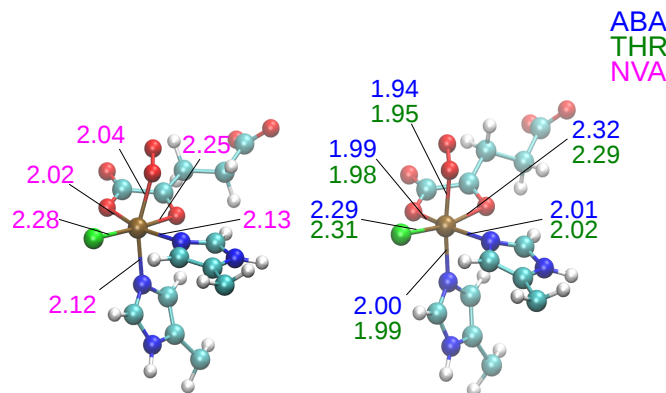


Figure S10: QM/MM-optimised structures of the O₂ complexes in the quintet state, ⁵B. Selected bond lengths are given in Å.

Table S8: Selected structural parameters of the O_2 complexes **B**. (*The structure of **THR-B** ($S = 1$) was optimised at def2-SVP level.)

Parameter	THR			ABA			NVA
	S=1*	S=2	S=3	S=1	S=2	S=3	S=2
Fe–N _{His235} (Å)	2.02	1.99	2.05	1.98	2.00	2.09	2.12
Fe–N _{His116} (Å)	2.11	2.02	2.12	2.00	2.01	2.11	2.13
Fe–Cl (Å)	2.32	2.31	2.27	2.24	2.29	2.24	2.28
Fe–O _P (Å)	2.01	1.95	2.22	1.95	1.94	2.13	2.04
Fe–O _{A1} (Å)	2.06	1.98	2.06	1.95	1.99	2.05	2.02
Fe–O _K (Å)	2.30	2.29	2.08	1.99	2.32	2.28	2.25
O–O (Å)	1.24	1.28	1.28	1.29	1.29	1.28	1.28
N _{His235} –Fe–O _P (°)	169	164	157	178	171	164	158

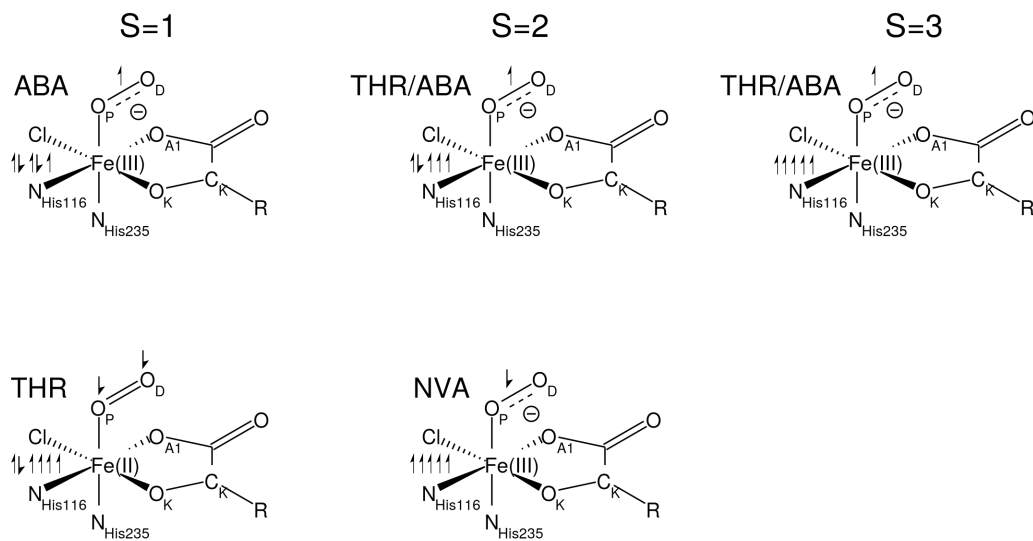


Figure S11: Schematic representation of the electronic structures of the O_2 complexes with $S = 1, 2, 3$. For **THR** and **ABA** ($S = 3$) and **NVA** ($S = 2$), the other direct donor atoms together carry another ~ 0.5 majority spins, which is included in the Fe spin count in the schematic.

2.3.2 O₂ complexes: QM/MM vs. HYSCORE

The pulsed-EPR (HYSCORE) experiments of Martinie *et al.*²³ provide distance and angle measurements between O_p, Fe, and specific hydrogens of the substrate; see Figure S12. In the experiment, NO is used as a non-reactive, EPR-active structural mimick of O₂, and substrates need to be deuterated at the position to be measured. Comparing to QM/MM-optimised structures, distances agree well, but angles do not (Table S12).

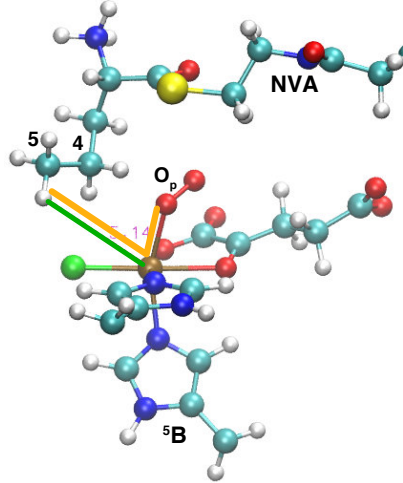


Figure S12: Structure of **NVA-⁵B**, with the Fe–(C⁵)H distance and the O_p–Fe–(C⁵)H angle highlighted in green and orange, respectively.

Table S9: Fe–H distances and O–Fe–H angles in O₂ complexes **B** from QM/MM optimisations and HYSCORE experiments²³.

		THR		ABA		NVA	
		(C ³)H	(C ⁴)H	(C ³)H	(C ⁴)H	(C ⁴)H	(C ⁵)H
Fe–H (Å)	QM/MM	4.42	4.11	4.3	3.9	3.2	5.14
	Expt	4.7 ± 0.4	4.2 ± 0.3	4.7 ± 0.3	3.7 ± 0.2	3.7 ± 0.3	3.4 ± 0.3
O _p –Fe–(C ³)H (°)	QM/MM	10	24	39	25	50	65
	Expt	81 ± 10	85 ± 10	85 ± 10	85 ± 10	64 ± 7	81 ± 15

2.3.3 O₂ activation/decarboxylation intermediates

Table S10: Selected structural parameters of intermediates along the O₂ activation/decarboxylation pathway, optimised at B3LYP-D3/def-TZVP/MM level. C² designates the keto-carbon of 2OG, labelled as C_K above. (*The structure of **THR**-³**B** was optimised at def2-SVP level.)

Substrate	Parameter	³ B	³ C1	³ C2a	³ D	⁵ B	⁵ C1	⁵ C2a	⁵ C2c	⁵ D	⁷ B	⁷ C2b	⁷ D
THR	Fe–N ₂₃₅ (Å)	2.05*	1.98	2.27	1.94	1.99	2.09	2.15	—	2.10	2.05	2.09	2.07
	Fe–N ₁₁₆ (Å)	2.12*	1.98	2.02	2.10	2.02	2.01	2.13	—	2.10	2.12	2.11	2.16
	Fe–Cl (Å)	2.27*	2.27	2.28	2.29	2.31	2.25	2.32	—	2.25	2.27	2.25	2.32
	Fe–O _p (Å)	2.22*	1.82	1.91	1.60	1.95	2.40	2.05	—	1.63	2.22	1.94	1.90
	Fe–O _k (Å)	2.08*	1.84	2.01	1.96	2.29	1.91	2.26	—	1.93	2.08	2.29	1.92
	O _p –O _d (Å)	1.28*	1.41	1.48	—	1.28	1.30	1.44	—	—	1.28	—	—
	O _d –C ² (Å)	2.57*	1.45	1.91	1.22	2.25	1.60	1.32	—	1.22	1.93	—	1.22
	N ₂₃₅ –Fe–O _p (°)	157*	171	165	111	164	157	114	—	95	157	155	106
ABA	Fe–N ₂₃₅ (Å)	1.98	—	—	2.08	2.00	2.11	2.12	2.10	2.07	2.09	2.11	2.07
	Fe–N ₁₁₆ (Å)	2.00	—	—	1.96	2.01	1.99	2.11	2.10	2.10	2.11	2.17	2.12
	Fe–Cl (Å)	2.24	—	—	2.33	2.29	2.26	2.35	2.33	2.26	2.24	2.24	2.36
	Fe–O _p (Å)	1.95	—	—	1.59	1.94	2.27	2.02	1.77	1.64	2.13	1.98	1.87
	Fe–O _k (Å)	1.99	—	—	1.99	2.32	2.01	2.33	2.17	1.94	2.28	2.21	1.95
	O _p –O _d (Å)	1.29	—	—	—	1.29	1.28	1.44	—	—	1.28	—	—
	O _d –C ² (Å)	2.23	—	—	1.23	2.47	2.07	1.32	—	1.22	2.43	—	1.23
	N ₂₃₅ –Fe–O _p (°)	178	—	—	156	171	169	139	127	93	164	166	101
NVA	Fe–N ₂₃₅ (Å)	—	—	—	—	2.12	—	2.10	—	2.05	—	—	—
	Fe–N ₁₁₆ (Å)	—	—	—	—	2.13	—	2.11	—	2.12	—	—	—
	Fe–Cl (Å)	—	—	—	—	2.28	—	2.37	—	2.29	—	—	—
	Fe–O _p (Å)	—	—	—	—	2.04	—	2.00	—	1.63	—	—	—
	Fe–O _k (Å)	—	—	—	—	2.25	—	2.33	—	1.95	—	—	—
	O _p –O _d (Å)	—	—	—	—	1.28	—	1.45	—	—	—	—	—
	O _d –C ² (Å)	—	—	—	—	2.47	—	1.32	—	1.22	—	—	—
	N ₂₃₅ –Fe–O _p (°)	—	—	—	—	158	—	132	—	96	—	—	—

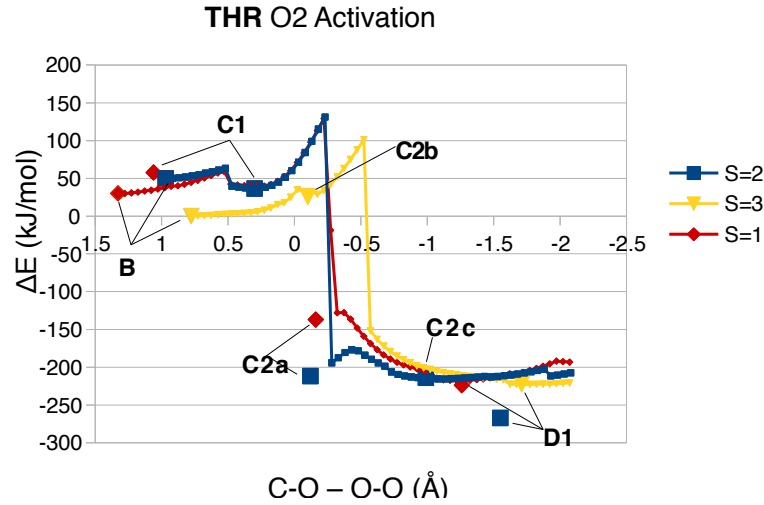


Figure S13: Energetic profiles of the reaction coordinate scans for **THR** on the triplet, quintet, and septet surfaces. Large, labelled symbols denote optimised intermediates. Scans and optimisations done at B3LYP-D3/def2-SVP/MM level.

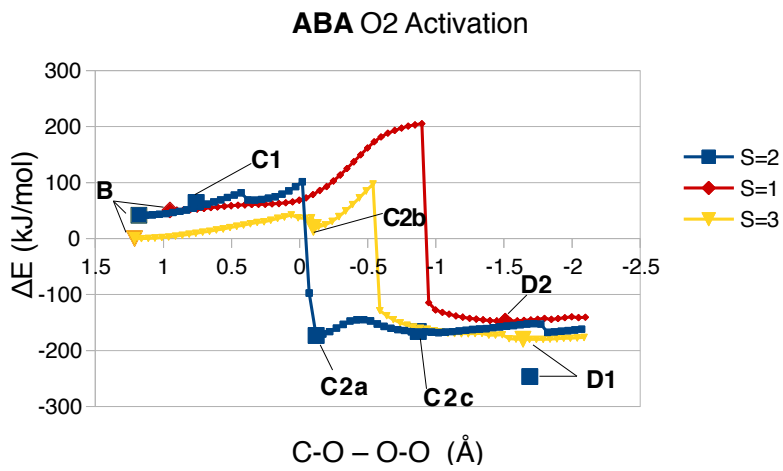


Figure S14: Energetic profiles of the reaction coordinate scans for **ABA** on the triplet, quintet, and septet surfaces. Large, labelled symbols denote optimised intermediates. Scans and optimisations done at B3LYP-D3/def2-SVP/MM level.

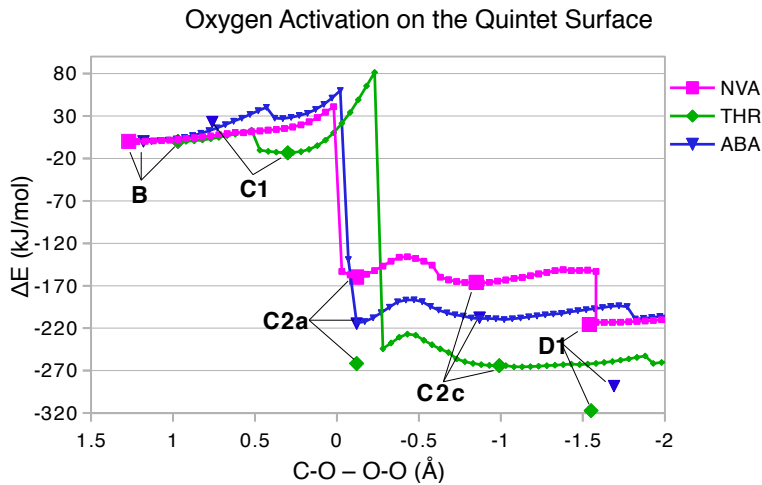


Figure S15: Energetic profiles of the reaction coordinate scans for **THR**, **ABA**, and **NVA** on the quintet surface. Large, labelled symbols denote optimised intermediates. Scans and optimisations done at B3LYP-D3/def2-SVP/MM level.

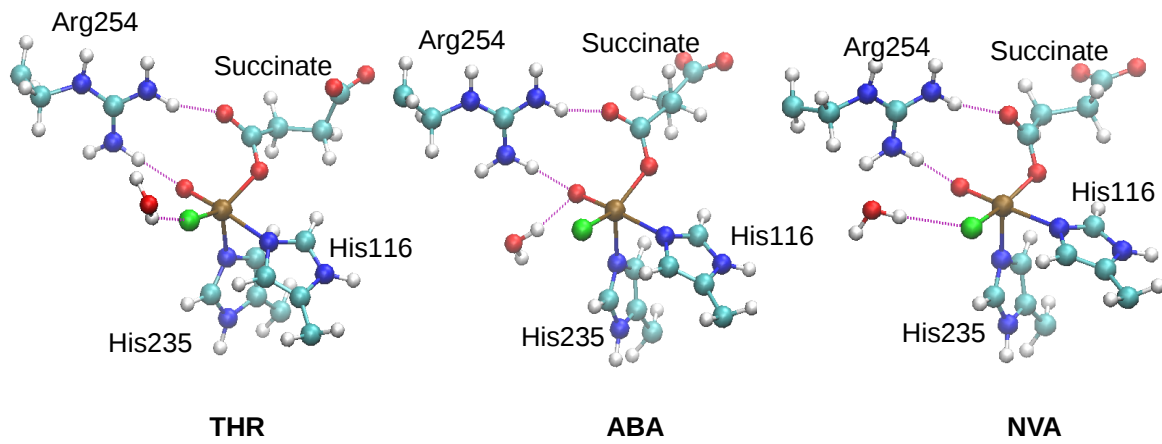


Figure S16: QM/MM-optimised structures of the preferred $[Fe=O]$ species, 5D1 , for the three substrates. In all three structures, Arg254 is hydrogen-bonding with one “arm” each to the oxido oxygen and the free carbonyl oxygen of the succinate ligand.

References

- [1] A. Jarnuczak, *MSci Thesis*, School of Chemistry, University of Glasgow, 2011.
- [2] A. Šali and T. L. Blundell, *J. Mol. Biol.*, 1993, **234**, 779–815.
- [3] *Modeller 9v8*, 2010.
- [4] A. Fiser, R. K. G. Do and A. Šali, *Protein Sci.*, 2000, **9**, 1753–1773.
- [5] J. Word, S. C. Lovell, J. S. Richardson and D. C. Richardson, *J. Mol. Biol.*, 1999, **285**, 1735–1747.
- [6] *Reduce 3.14*, 2010.
- [7] V. B. Chen, W. B. Arendall, J. J. Headd, D. A. Keedy, R. M. Immormino, G. J. Kapral, L. W. Murray, J. S. Richardson and D. C. Richardson, *Acta Crystallogr. Sect. D-Biol. Crystallogr.*, 2009, **66**, 12–21.
- [8] H. Li, A. D. Robertson and J. H. Jensen, *Proteins: Struct., Funct., Bioinf.*, 2005, **61**, 704–721.
- [9] *PropKa 2.0*, 2008.
- [10] U. C. Singh and P. A. Kollman, *J. Comput. Chem.*, 1984, **5**, 129–145.
- [11] Y. Duan, C. Wu, S. Chowdhury, M. C. Lee, G. Xiong, W. Zhang, R. Yang, P. Cieplak, R. Luo, T. Lee, J. Caldwell, J. Wang and P. Kollman, *J. Comput. Chem.*, 2003, **24**, 1999–2012.
- [12] O. Treutler and R. Ahlrichs, *J. Chem. Phys.*, 1995, **102**, 346–354.
- [13] M. Von Arnim and R. Ahlrichs, *J. Comput. Chem.*, 1998, **19**, 1746–1757.
- [14] TURBOMOLE V6.4 2012, a development of University of Karlsruhe and Forschungszentrum Karlsruhe GmbH, 1989–2007, TURBOMOLE GmbH, since 2007; available from <http://www.turbomole.com>.
- [15] M. J. Frisch, G. W. Trucks, H. B. Schlegel, G. E. Scuseria, M. A. Robb, J. R. Cheeseman, G. Scalmani, V. Barone, B. Mennucci, G. A. Petersson, H. Nakatsuji, M. Caricato, X. Li, H. P. Hratchian, A. F. Izmaylov, J. Bloino, G. Zheng, J. L. Sonnenberg, M. Hada, M. Ehara, K. Toyota, R. Fukuda, J. Hasegawa, M. Ishida, T. Nakajima, Y. Honda, O. Kitao, H. Nakai, T. Vreven, J. A. Montgomery, Jr., J. E. Peralta, F. Ogliaro, M. Bearpark, J. J. Heyd, E. Brothers, K. N. Kudin, V. N. Staroverov, R. Kobayashi, J. Normand, K. Raghavachari, A. Rentell, J. C. Burant, S. S. Iyengar, J. Tomasi, M. Cossi, N. Rega, J. M. Millam, M. Klene, J. E. Knox, J. B. Cross, V. Bakken, C. Adamo, J. Jaramillo, R. Gomperts, R. E. Stratmann, O. Yazayev, A. J. Austin, R. Cammi, C. Pomelli, J. W. Ochterski, R. L. Martin, K. Morokuma, V. G. Zakrzewski, G. A. Voth, P. Salvador, J. J. Dannenberg, S. Dapprich, A. D. Daniels, O. Farkas, J. B. Foresman, J. V. Ortiz, J. Cioslowski and D. J. Fox, *Gaussian 09 Rev. A.02*, Gaussian Inc., Wallingford, CT, 2009.
- [16] H. M. Senn, S. Thiel and W. Thiel, *J. Chem. Theory Comput.*, 2005, **1**, 494–505.
- [17] S. K. Schiferl and D. C. Wallace, *J. Chem. Phys.*, 1985, **83**, 5203–5209.
- [18] J. Kästner, S. Thiel, H. M. Senn, P. Sherwood and W. Thiel, *J. Chem. Theory Comput.*, 2007, **3**, 1064–1072.
- [19] E. Chovancova, A. Pavelka, P. Benes, O. Strnad, J. Brezovsky, B. Kozlikova, A. Gora, V. Sustr, M. Klvana, P. Medek, L. Biedermannova, J. Sochor and J. Damborsky, *PLoS Comput. Biol.*, 2012, **8**, e1002708.
- [20] M. Matthews, C. Krest, E. Barr, F. Vaillancourt, C. Walsh, M. Green, C. Krebs and J. Bollinger Jr, *Biochemistry*, 2009, **48**, 4331–4343.
- [21] S. D. Wong, M. Srnec, M. L. Matthews, L. V. Liu, Y. Kwak, K. Park, C. B. Bell III, E. E. Alp, J. Zhao, Y. Yoda, S. Kitao, M. Seto, C. Krebs, J. M. Bollinger and E. I. Solomon, *Nature*, 2013, **499**, 320–323.
- [22] T. Borowski, H. Noack, M. Radoñ, K. Zych and P. E. M. Siegbahn, *J. Am. Chem. Soc.*, 2010, **132**, 12887–12898.
- [23] R. J. Martinie, J. Livada, W. C. Chang, M. T. Green, C. Krebs, J. Bollinger, J. M. and A. Silakov, *J. Am. Chem. Soc.*, 2015, **137**, 6912–6919.